Anomalous Josephson Current in Junctions with Spin Polarizing Quantum Point Contacts

A. A. Reynoso,[1,2] Gonzalo Usaj,[1,2] C. A. Balseiro,[1,2] D. Feinberg,[3] and M. Avignon[3]

[1]*Instituto Balseiro, Centro Atómico Bariloche, Río Negro, Argentina*
[2]*Consejo Nacional de Investigaciones Científicas y Técnicas (CONICET), Argentina*
[3]*Institut NEEL, CNRS and Université Joseph Fourier, Boite Postale 166, 38042 Grenoble, France*

(Received 7 May 2008; published 2 September 2008)

We consider a ballistic Josephson junction with a quantum point contact in a two-dimensional electron gas with Rashba spin-orbit coupling. The point contact acts as a spin filter when embedded in a circuit with normal electrodes. We show that with an in-plane external magnetic field an anomalous supercurrent appears even for zero phase difference between the superconducting electrodes. In addition, the external field induces large critical current asymmetries between the two flow directions, leading to supercurrent rectifying effects.

DOI: 10.1103/PhysRevLett.101.107001 PACS numbers: 74.45.+c, 71.70.Ej, 72.25.Dc, 74.50.+r

Josephson junctions (JJ) are the basic building blocks for superconducting electronics with applications that range from SQUID magnetometers to possible quantum computing devices. In superconductor-normal metal-superconductor (S-N-S) junctions the supercurrent flow is due to the Andreev states—a coherent superposition of electron and holes states. These states depend on the electronic structure of the normal material and on the properties of the S-N interface [1–4]. Modern technologies based on two-dimensional electron gases (2DEGs) [5,6] or nanowires [7] allow for a precise control of such electronic properties, and thus of the JJ characteristics. Moreover, spin-orbit (SO) effects offer new alternatives to control the spin and charge transport [8,9].

Superconducting rectifiers are among the new devices proposed and studied during the last few years. Most of these proposals are based on the dynamics of vortices [10,11]. Here we show that in systems with SO coupling rectifying properties can be obtained by controlling the spin of the Andreev states. To this end we consider a ballistic JJ with a quantum point contact (QPC) in a 2DEG with SO interaction. The QPC can be tuned to control the number of transmitting channels and thus the critical current of the junction [3–5,12,13]. On the other hand, the QPC with SO coupling may act as a spin filter producing spin-polarized currents when embedded in a circuit with normal leads [14–16]. The normal current also generates an in-plane magnetization—perpendicular to the current—as well as out-of-plane spin-Hall textures [17]. Both effects are maximized at the core of the QPC [18]. As the SO-coupling preserves time-reversal symmetry (TRS), we expect that these peculiarities of the transmitting channels do not harm the Josephson effect when the leads become superconducting. However, the Josephson current itself breaks the TRS and, as we show below, it reveals striking effects of the SO-coupling. For example, the supercurrent generates spin polarization in the 2DEG [19] and the QPC in a similar way normal current does [17,18]. This is due to the distinctive spin texture of each Andreev state that contributes to the local magnetization in a supercurrent-carrying state.

More striking effects take place if an external in-plane magnetic field is applied. Its effect on the supercurrent characteristics depends on the nature of the junction. In the absence of SO-coupling, the Zeeman field may generate π-junctions resembling the case of S-ferromagnet-S junctions [1,20]. For systems with SO-coupling, the existing theories include the description of perfectly contacted 2DEG junctions [21], wide junctions [22], 1D-conductors [23] and junctions with quantum dots [24,25]. In our case, the QPC, the internal SO field and the external Zeeman field conspire to reveal novel effects. Remarkably, we find a critical current I_c that depends on the current flow direction. With more than one transmitting channel, the QPC can be tuned to show either a large I_c asymmetry or a perfect symmetry. In this regime the JJ can act as a supercurrent rectifier [10,11]. At the origin of this effect is the anomalous supercurrent—proportional to the external field—that appears even for zero phase difference ϕ between the two superconducting leads [20,23]. Devices based on InAs-related materials, that present strong gate-tunable Rashba SO-coupling are good candidates to look for these effects [5,6]. In what follows we present the main results of the theory.

The total Hamiltonian of the system reads

$$H = H_{\mathrm{QPC}} + H_R + H_L + H_C, \tag{1}$$

here H_{QPC} describes the central 2DEG with the QPC [see Fig. 1(a)]. In the effective mass approximation $H_{\mathrm{QPC}} = (p_x^2 + p_y^2)/2m^* + \alpha/\hbar(p_y\sigma_x - p_x\sigma_y) + V(x,y) - g\mu_B\vec{\sigma}\cdot B$, where the first two terms are the kinetic energy and the Rashba SO-coupling, respectively, and $V(x,y)$ is the confinement potential that defines the QPC. We use a potential that simulates the effect of two electrodes held at a distance z from the 2DEG [26], with a gate voltage controlling the height, V_g, of the potential barrier at the center of the QPC. The last term in H_{QPC} is the Zeeman energy. The Hamiltonians H_R and H_L describe the right and left

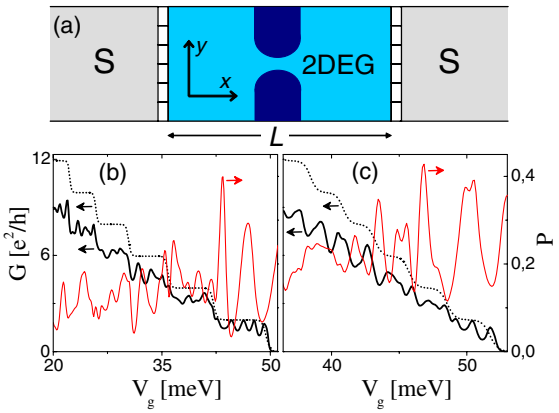

FIG. 1 (color online). (a) Schematic view of the junction. Panels (b) and (c) correspond to QPC1 and QPC2 simulated with gates placed at $z = 30$ and 90 nm on top of the 2DEG, respectively. The conductance with ideal 2DEG electrodes (dotted line), with the metallic electrodes described in the text (thick line) and the current polarization P (thin line) are shown. The Rashba coupling strength is $\alpha = 20$ meV nm.

superconducting electrodes with an order parameter $\Delta_{R/L} = \Delta_0 e^{\pm i\phi/2}$. Finally, H_C describes the contact between the superconductors and the 2DEG.

For the numerical calculations we discretize the space, mapping the Hamiltonian (1) onto a tight-binding-like model. We use a square lattice with hopping matrix elements t_N and t_S for the normal (2DEG) and superconducting materials, respectively [27]. The microscopic parameters of the normal region correspond to InAs-like materials [5]: the effective mass is $m^* = 0.045 m_e$ and the electron density $n \sim 10^{12}$ cm^{-2} (the Fermi energy is $E_F \sim 53$ meV). We take the total length of the junction $L = 1.2$ μm and analyze two point contacts denoted as QPC1 and QPC2 corresponding to different values of z. We use $\Delta_0 = 1.5$ meV and the coherent length $\xi_0 = \hbar v_F^s/\Delta_0 = 43$ nm corresponding to Nb films, v_F^s is the Fermi velocity of the superconductor [5,6].

We calculate the normal and anomalous propagators that contain the information of all the physical quantities of interest. For $\Delta_0 = 0$ the normal conductance $G = \sum_{\sigma,\sigma'} G_{\sigma,\sigma'}$ is evaluated using the conventional Landauer-like formulation [26]. Here $G_{\sigma,\sigma'}$ is the contribution to the conductance due to incident electrons with spin σ that are transmitted with spin σ'. The spin polarization of the current is defined as $P = \sum_\sigma (G_{\sigma,\uparrow} - G_{\sigma,\downarrow})/G$. These quantities characterize the QPC in the normal state. For $\Delta_0 \neq 0$ we calculate the Josephson current flowing through the right N-S interface, [27]

$$I(\phi) = i\frac{e}{\hbar} \sum_{i\in N, j\in S} [t_{SN}^{i,j} \langle \psi^\dagger(x_j)\psi(x_i)\rangle - t_{SN}^{j,i} \langle \psi^\dagger(x_i)\psi(x_j)\rangle]. \quad (2)$$

Here x_i and x_j are coordinates at the edge of the 2DEG and the superconducting electrode, respectively, $t_{SN}^{i,j}$ is the hopping matrix element connecting neighboring sites at the interface and the field operator $\psi^\dagger(x) = (\psi_\uparrow^\dagger(x), \psi_\downarrow^\dagger(x))$ creates an electron at coordinate x. We choose $t_{SN}^{i,j} = (t_N + t_S)/2$; decreasing this value increases the normal scattering at the interface producing narrow resonances within the central 2DEG region with strong influence on the Josephson current [13].

The zero-field case.—The normal conductance of the system presents clear structures on top of the plateaus [see Figs. 1(b) and 1(c)] due to broad resonances originated in the scattering at the electrode-2DEG interfaces. As shown in the same figure these QPCs generate spin-polarized currents with a polarization P in the range (0–0.6) depending on the strength of the SO-coupling and the number of transmitting channels.

For superconducting contacts, the current-phase relation (CPR) is shown in Fig. 2(a) for different values of the parameters. We observe two characteristic CPR: resonant-like and tunnelinglike (sinusoidal) relations. As V_g changes, the junction alternates between these two behaviors. The critical current I_c is defined as the maximum current in the CPR. The dependence of I_c and the conductance of the normal state G on V_g is shown in Fig. 2(b). The structure of both curves is similar with the peaks located at the same position showing that the maximums of I_c are due to one-electron resonances [4]. The structure of the Andreev spectrum includes a number of (dispersive) states with phase-dependent energies and (nondispersive) states confined at each side of the constriction; details will

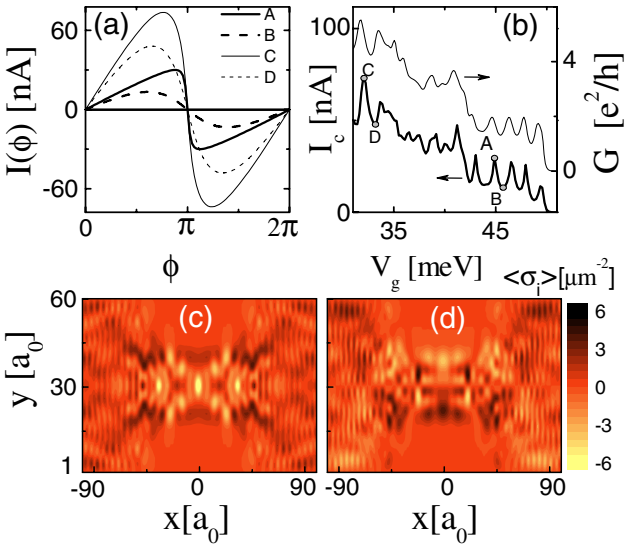

FIG. 2 (color online). (a) Current-phase relation (CPR) for different gate voltages in QPC1. (b) Critical current and conductance as function of V_g. The points labeled with letters indicate the parameters of the curves of panel (a). In (c) and (d) color maps of the y and z magnetization calculated with the critical current of curve C of panel (a) are shown. The SO strength is $\alpha = 20$ meV $\cdot$ nm and the lattice parameter is $a_0 = 3$ nm.

be presented elsewhere [28]. When there is only one transmitting channel, the Josephson current is dominated by a single (spin) pair of dispersive Andreev states. As V_g decreases and the QPC opens, the current is the superposition of contributions due to different pairs of states.

Because of the SO-coupling each Andreev state has a well-defined spin texture which in the presence of a supercurrent contributes to the local magnetization. As an illustration we calculate the magnetization components $\langle S_y(x_i)\rangle$ and $\langle S_z(x_i)\rangle$ for all the lattice sites within the 2DEG. As shown in Figs. 2(c) and 2(d), the supercurrent-induced steady magnetization has an in-plane component perpendicular to the current direction and an out-of-plane component with the spin-Hall structure [17,19].

Effect of external in-plane magnetic fields.—The spin texture of each Andreev state has a component along the y direction. In general, for spin-polarizing QPCs, a pair of dispersive Andreev states—indicated by $|+\rangle$ and $|-\rangle$—have $\langle +|S_y|+\rangle \neq -\langle -|S_y|-\rangle$. Consequently, with an external field B in the y direction the absolute value of their Zeeman shifts are different. The effect is illustrated in Figs. 3(a) and 3(b). In QPCs with a single transmitting channel we follow a resonance as the SO-coupling α is increased. For small α we observe the characteristic behavior of a resonant state in the presence of a field. The distance between the steplike changes of the current is a measure of the Zeeman splitting. As α increases the Zeeman shift of one of the Andreev states decreases and changes sign (the steplike structure crosses the $\phi = \pi$ point). In the large α limit $\langle +|S_y|+\rangle \approx \langle -|S_y|-\rangle$ and the CPR shows a single step. In this limit, the QPC acts as a very efficient spin filter in the first plateau [14,18]: all transmitted electrons have essentially the same spin orientation. This results in an anomalous supercurrent for $\phi = 0$. To estimate it, we may assume a smooth QPC and evaluate the phase shift $\vartheta_n(E)$ acquired by an electron traveling from one superconducting electrode to the other in the WKB approximation. In $\vartheta_n(E)$ the index $n = \pm$ is the channel index and E is the energy measured from the Fermi energy. For small E we have

$$\vartheta_n(E) \approx k_F \lambda_n + \frac{E}{\hbar v_F}\delta_n; \tag{3}$$

here k_F (v_F) is the Fermi wave vector (velocity) in the 2DEG, $\lambda_n \lesssim L$ and $\delta_n \gtrsim L$ are related to the effective length of the junction at the Fermi energy. Assuming that at resonance the scattering at SN interface plays no important role we have [23]

$$I(\phi) = \frac{e v_F}{\pi}\sum_n \frac{1}{\delta_n}\Omega\left(\phi + \mu_n \frac{B}{\Delta_n}\right); \tag{4}$$

here $\Omega(x)$ is a periodic function with $\Omega(x) = x$ for $|x| < \pi$, $\Delta_n = \hbar v_F/\delta_n$ and $\mu_n B$ is the Zeeman shift. Then, in Figs. 3(a) and 3(b) the steplike structures correspond to $\phi = \pi - \mu_n B/\Delta_n$ and the anomalous current $I(0) = (2e/h)\sum_n \mu_n B$ is given by the total Zeeman energy of the transmitting channels—note it does not depend on L. Nonlinear effects with larger anomalous currents occur for large fields if $\mu_n B/\Delta_n > \pi$ for some of the channels. We consider only the linear regime in which the current cancels for a phase $\varphi = \pi I(0)\delta_+\delta_-/e v_F(\delta_+ + \delta_-)$. This φ-junction in a ring geometry generates a spontaneous current with a fraction of a vortex threading the ring. Let us point out that the Zeeman field couples to the momentum through the SO-coupling, acting as a gauge field that generates a φ-junction. Yet, this kind of symmetry argument is not sufficient, and the adiabatic QPC here plays an essential role in filtering and coherently mixing very few transverse channels. Indeed, no such effects have been obtained in wide junctions [21] and quantum dots [24]. An exception is Ref. [23], where a 1D case was considered.

As in the zero-field case, a small change in V_g shifts the resonance from E_F and the current becomes a smooth function of the phase, characteristic of a nonresonant junction. Remarkably, with more than one pair of transmitting channels the CPR presents new effects, displayed for instance in the second conductance plateau; Figs. 3(c) and 3(d). In Fig. 3(c), we show a value of V_g for which two resonances—with different values of their parameters μ_n and δ_n-lie at E_F. Changing V_g shifts each resonance by a different amount. The total CPR now results from the superposition of contributions with different steplike structures and different φ-shifts. This leads to a critical current I_c that depends on the current direction. We define the critical current asymmetry as I_c^+/I_c^- where I_c^+ and I_c^- are the critical currents for each flow direction. Figure 4 shows that for physical values of the parameters a large asymmetry can be obtained by tuning the gate voltage. The magnitude of the asymmetry depends on the detailed structure of the dispersive Andreev states, which is determined by the interplay between the SO coupling, the external field and the QPC potential [see Figs. 4(c) and 4(d)]. We found that

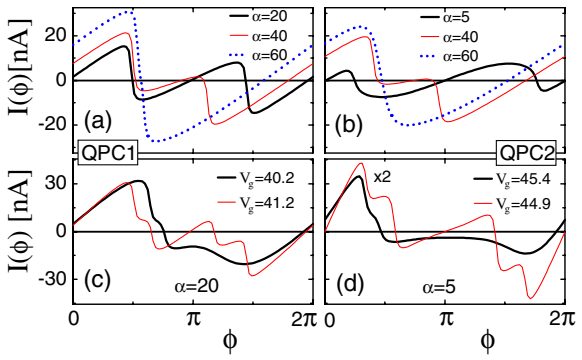

FIG. 3 (color online). CPR for QPC1 [panels (a) and (c)] and QPC2 [panels (b) and (d)] with an external field of $g\mu_B B = 0.3$ meV. In (a) and (b) the QPC height V_g is set to follow a resonance at the first conductance plateau for different values of the SO coupling α (in meVnm). In (c) and (d) the $I(\phi)$ for different V_g (in meV) at the second and third plateaus are shown. Note the asymmetry between $I(\phi) > 0$ and $I(\phi) < 0$.

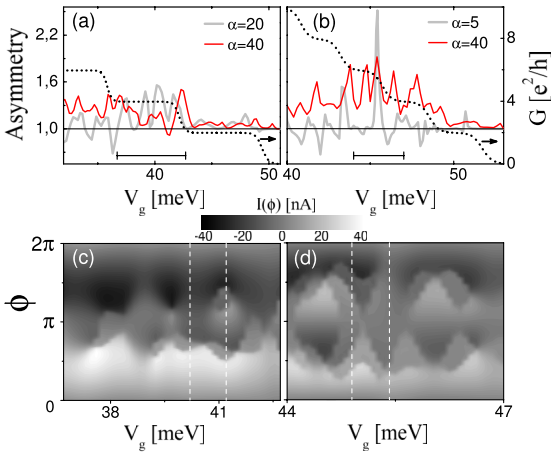

FIG. 4 (color online). Critical current asymmetry vs V_g for QPC1 (a) and QPC2 (b) and different values of α (in meVnm) with the same applied field of Fig. 3. The conductance of the QPCs is also shown (dotted line). The lower panels are maps of the supercurrent for QPC1 with $\alpha = 20$ (c) and QPC2 with $\alpha = 5$ (d) in the $[\phi, V_g]$ plane. The V_g-scales of these maps are shown with horizontal bars in panels (a) and (b). The vertical dashed lines correspond to the curves of Figs. 3(c) and 3(d).

the asymmetry I_c^+/I_c^- can be larger than 3. These large asymmetry values are the main result of our work.

In summary, we have shown that a spin-polarizing QPC brings new physics to the JJs. While the most relevant effect is the new mechanism to generate critical current asymmetries, the device shows other interesting properties that highlight the effects of the SO-coupling on the Andreev states: (i) the supercurrent generates a magnetization in the 2DEG, being larger at the core of the QPC; (ii) an external in-plane magnetic field induces an anomalous current at zero phase difference (a φ-junction) [23]. In the latter case, we obtain π-junctions for some values of the gate voltage (as for $\alpha = 0$), while in general $\varphi < \pi$. Such junctions, tunable both by an external flux and a Zeeman field, may have applications in SQUIDs or superconducting quantum bits. With more than one transmitting channel, the external field induces a large critical current asymmetry if the QPC potential V_g is properly tuned. Even for moderate values of the SO-coupling, and realistic values of the external field ($B < 1$ T), the asymmetry can be quite large. The QPC is a central ingredient as it allows the control of the number and properties of the transmitting channels. These junctions act as supercurrent rectifiers in the interval $\min(I_c^+, I_c^-) < |I| < \max(I_c^+, I_c^-)$, which can be controlled by adjusting the gate voltage. As this effect relies on the control of the spin polarization of the Andreev states, it generates a new alternative for supercurrent rectifiers based on pure spintronic effects.

We acknowledge financial support through the ECOS-SECyT collaboration program A06E03, ANPCyT Grants No. 13829 and 13476 and CONICET PIP 5254. AAR and GU acknowledge support from CONICET. DF and MA acknowledge support from ANR PNano Grant 050-S2.

[1] A. A. Golubov, M. Yu. Kupriyanov, and E. Ilichev, Rev. Mod. Phys. **76**, 411 (2004).
[2] K. K. Likharev, Rev. Mod. Phys. **51**, 101 (1979).
[3] C. W. J. Beenakker and H. van Houten, Phys. Rev. Lett. **66**, 3056 (1991); C. W. Beenakker, Phys. Rev. Lett. **67**, 3836 (1991).
[4] A. Furusaki, H. Takayanagi, and M. Tsukada, Phys. Rev. Lett. **67**, 132 (1991); Phys. Rev. B **45**, 10 563 (1992).
[5] H. Takayanagi, T. Akazaki, and J. Nitta, Phys. Rev. Lett. **75**, 3533 (1995).
[6] M. Ebel, C. Busch, U. Merkt, M. Grajcar, T. Plecenik, and E. Il'ichev, Phys. Rev. B **71**, 052506 (2005); E. Giazotto *et al.*, J. Supercond. **17**, 317 (2004); P. Baars, A. Richter, and U. Merkt, Phys. Rev. B **67**, 224501 (2003).
[7] Y. J. Doh, J. A. van Dam, A. L. Roest, E. P. A. M. Bakkers, L. P. Kouwenhoven, and S. De Franceschi, Science **309**, 272 (2005).
[8] R. Winkler, *Spin-Orbit Coupling Effects in Two-Dimensional Electron and Hole Systems* (Springer, New York, 2003).
[9] *Semiconductor Spintronics and Quantum Computation*, edited by D. Awschalom, N. Samarth, and D. Loss (Springer, New York, 2002).
[10] I. Zapata, R. Bartussek, F. Sols, and P. Hänggi, Phys. Rev. Lett. **77**, 2292 (1996).
[11] G. Carapella and G. Costabile, Phys. Rev. Lett. **87**, 077002 (2001).
[12] C. J. Muller, J. M. van Ruitenbeek, and L. J. de Jongh, Phys. Rev. Lett. **69**, 140 (1992).
[13] D. D. Kuhn, N. M. Chtchelkatchev, G. B. Lesovik, and G. Blatter, Phys. Rev. B **63**, 054520 (2001).
[14] M. Eto, T. Hayashi, and Y. Kurotani, J. Phys. Soc. Jpn. **74**, 1934 (2005).
[15] P. G. Silvestrov and E. G. Mishchenko, Phys. Rev. B **74**, 165301 (2006).
[16] A. Reynoso, G. Usaj, and C. A. Balseiro, Phys. Rev. B **75**, 085321 (2007).
[17] G. Usaj and C. A. Balseiro, Europhys. Lett. **72**, 631 (2005).
[18] A. Reynoso, G. Usaj, and C. A. Balseiro, Physica (Amsterdam) **384B**, 28 (2006).
[19] A. G. Mal'shukov and C. S. Chu, arXiv:0801.4419 [Phys. Rev. B (to be published)].
[20] A. I. Buzdin, Rev. Mod. Phys. **77**, 935 (2005); A. I. Buzdin, Phys. Rev. B **72**, 100501 (2005).
[21] E. V. Bezuglyi, A. S. Rozhavsky, I. D. Vagner, and P. Wyder, Phys. Rev. B **66**, 052508 (2002).
[22] O. V. Dimitrova and M. V. Feigel'man, JETP **102**, 652 (2006).
[23] I. V. Krive, S. I. Kulinich, R. I. Shekhter, and M. Jonson, Low Temp. Phys. **30**, 554 (2004); I. V. Krive, A. M. Kadigrobov, R. I. Shekhter, and M. Jonson, Phys. Rev. B **71**, 214516 (2005).
[24] L. Dell'Anna, A. Zazunov, R. Egger, and T. Martin, Phys. Rev. B **75**, 085305 (2007).
[25] B. Béri, J. H. Bardarson, and C. W. Beenakker, Phys. Rev. B **77**, 045311 (2008).
[26] D. K. Ferry and S. M. Goodnick, *Transport in Nanostructures* (Cambridge University Press, New York, 1997).
[27] J. C. Cuevas, A. Martín-Rodero, and A. Levy Yeyati, Phys. Rev. B **54**, 7366 (1996).
[28] A. A. Reynoso *et al.* (to be published).